Investigations of the Adsorption of *n*-Pentane in Several Representative Zeolites

Haiyan Wang, Elizabeth A. Turner, and Yining Huang*

Department of Chemistry, The University of Western Ontario, London, Ontario, Canada N6A 5B7

Received: February 6, 2006; In Final Form: March 14, 2006

We have examined the adsorption of *n*-pentane in several representative zeolites such as silicalite (MFI), ferrierite (FER), zeolite L (LTL), and faujasite zeolites with FAU structure including siliceous Y (Si−Y) and Na−Y by using FT-Raman spectroscopy in combination with thermogravimetric analysis (TGA) with particular attention being paid to the conformational and dynamic behavior of the guest molecule. The results indicate that the framework topology mainly dictates the conformation of *n*-pentane in a zeolite. For the zeolites with channel systems such as silicalite, ferrierite, and zeolite L, the population of the *all-trans* conformer increases upon loading, given that the geometry of the isomer fits better in the channel. When *n*-pentane is adsorbed in zeolites with a large cavity, such as Si−Y and Na−Y, the distribution of the *all-trans* (TT) and *trans-gauche* (TG) conformers is similar to that of pure liquid, suggesting that the large supercage in the framework imposes minimal effect on the conformational equilibrium. The dynamics of the guest molecule is, however, influenced significantly by the existence of cations. Adsorption of *n*-pentane in a siliceous framework such as silicalite and Si−Y results in extensive molecular motion at room temperature, the degree of which decreases with decreasing temperature. In zeolites ferrierite, L, and Na−Y, the presence of cations in the framework markedly hinders the overall molecular motion. The cations clearly play a role in the observed static disorder of the guest molecule in zeolite L. Important information regarding the location of the *n*-pentane molecules within silicalite and ferrierite is also obtained.

Introduction

Zeolites are crystalline microporous materials composed of corner and edge sharing AlO_4 and SiO_4 tetrahedra. These materials have three-dimensional frameworks, which contain channels or cages that are accessible to various guest molecules.[1] Zeolites are widely used in industry as catalysts, sorbents, and ion exchangers. Most applications of zeolites involve incorporating guest molecules into their frameworks, therefore, it is important to understand the behavior of the adsorbed molecules inside zeolite hosts. The conformational and dynamic behavior of adsorbed molecules within zeolites is fundamentally important because the behavior of this type can have a significant effect on the adsorption and diffusion properties of guest molecules as well as the subsequent chemistry within these systems. Detailed knowledge of the adsorption of *n*-alkanes in zeolites is of considerable practical interest in petrochemical applications, since zeolites are widely employed for acid-catalyzed reactions involving *n*-alkanes.[2] Adsorption of *n*-alkanes in zeolites has been the subject of a large number of studies;[3−5] however, most of these studies are computational simulations.[3] Experimentally, the majority of this research involves thermodynamic studies such as adsorption and desorption isotherms.[4] Little information regarding the conformational and dynamic behavior of adsorbed *n*-alkane molecules inside zeolites is available at a molecular level.[5]

In this work, we have used FT-Raman spectroscopy in combination with thermogravimetric analysis (TGA) to investigate the adsorptive properties of *n*-pentane in several representative zeolite frameworks. TGA is used to estimate the number of adsorption sites and the distribution of the guest molecules over these sites. FT-Raman spectroscopy is a useful technique for investigating conformational behavior and the local environments of molecules adsorbed inside the framework of zeolites via monitoring the guest molecules.[6] Zeolites exhibit weak Raman signals as a result of their intrinsically small Raman scattering cross sections. This is advantageous in the investigation of the behavior of sorbate inside a zeolite. The weak background of zeolites allows the Raman signals of adsorbed molecules to be detected. This technique has the ability to detect subtle structural changes in the guest molecules within the zeolitic framework by monitoring spectral parameters such as band splitting, peak intensity, line width, and frequency shift of the guest molecules. Furthermore, Raman spectroscopy has a fast time scale, therefore, the separate peaks due to different conformers can be observed simultaneously under favorable conditions. The Fourier transform (FT)-Raman technique[7] is particularly advantageous compared to conventional visible Raman. This is because FT-Raman instrumentation uses the 1064-nm excitation line from a near-infrared laser that significantly reduces the fluorescence background (a problem often associated with zeolites). The low energy of the excitation also minimizes laser induced desorption.

Experimental Section

Silicalite was prepared according to a procedure previously described.[8] Ferrierite (Si/Al = 9.1) and zeolite L (Si/Al = 3.05) were obtained from TOSOH corporation. Zeolites Si−Y (Si/Al=300) and Na−Y (Si/Al=2.35) were obtained from Degussa and Strem Chemicals, respectively. The purity and crystallinity of the zeolites were confirmed by powder X-ray diffraction. *n*-Pentane (99%) was obtain from Aldrich Chemical Co. and used without further purification.

* Address correspondence to this author. E-mail yhuang@uwo.ca. Phone: 519-661-2111 ext 86384. Fax: 519-661-3022.

10.1021/jp060775f CCC: $33.50
Published on Web 04/20/2006

SCHEME 1: The Three Conformers of *n*-pentane: (A) *all-trans* (TT); (B) *trans-gauche* (TG), and (C) *gauche-gauche* (GG)′

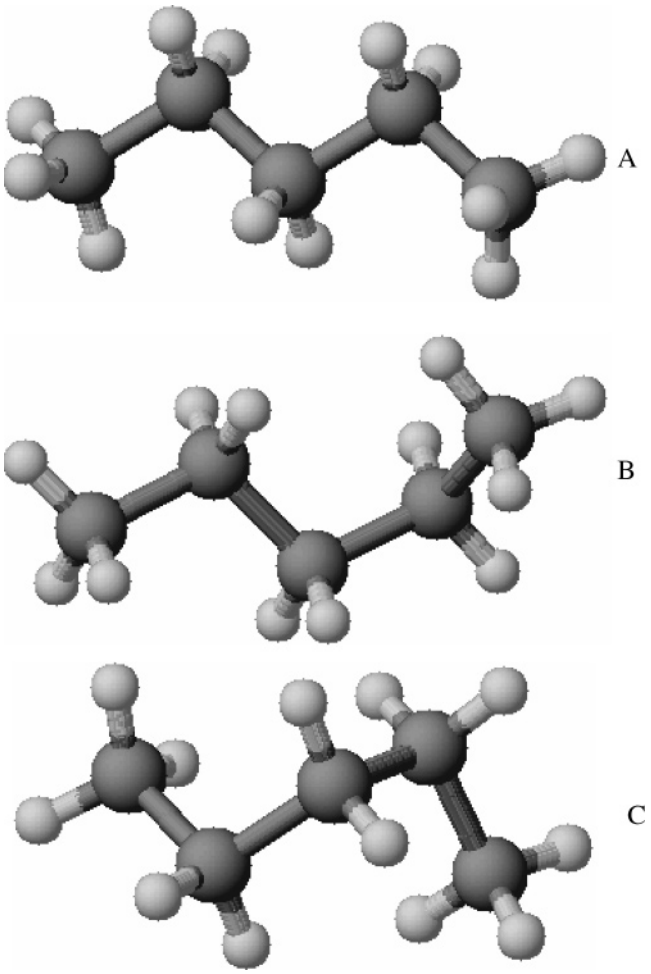

Precisely measured aliquots of *n*-pentane were added to accurately weighed zeolite powders (which were carefully dehydrated) in a glass tube. The glass tubes were immediately sealed and left overnight at room temperature to allow the sorbate molecules to disperse uniformly throughout the sample (since the boiling point of *n*-pentane is low, no heating is needed). The loading of *n*-pentane was confirmed by TGA.

All Raman spectra were recorded on a Bruker RFS 100/S spectrometer equipped with a Nd^{3+}:YAG laser operating at 1064.1 nm, and a liquid nitrogen cooled Ge detector. The laser power was typically 100 mW at the sample and the resolution was 2 cm^{-1}. Low-temperature measurements were carried out by using a Bruker Eurotherm 800 series temperature control unit, which regulated the sample temperature within ±1 °C. TGA measurements were performed on a Mettler Toledo TGA/SDTA851[e] analyzer with a temperature range of 25−500 °C at a heating rate of 10 °C/min.

Results and Discussion

In pure liquid, *n*-pentane exists in a dynamic mixture of three distinct conformers including the straight chain *all-trans* isomer and kinked chain conformers with up to two gauche bonds (Scheme 1). Much effort has been devoted to the conformational analysis of pure *n*-pentane by electron diffraction,[9] theoretical calculations,[10] and in particular vibrational studies.[11] The concentrations of different conformers in liquid *n*-pentane at room temperature are approximately 47%, 51%, and 2% for *all-trans* (TT), *trans-gauche* (TG), and *gauche-gauche* (GG), respectively.[10a] Raman spectra reported in the literature show that the intensities of the peaks associated with TT and TG conformers are very strong.[11d,f] Thus, these are the two major conformers that were examined in the present study. The intensity of the bands associated with the GG conformer is rather weak due to its low concentration. Previous IR and Raman studies have shown that in the solid state, *n*-pentane molecules exist exclusively in the *all-trans* form as the vibrational bands assigned to the gauche forms disappear upon crystallization.[11a,b,c] To assist in interpreting the data, the spectra of both liquid and solid *n*-pentane were recorded at room temperature and 140 K, respectively (Figure 1A,B), and are in good agreement with those reported in the literature.[11d] The spectral assignments of *n*-pentane were based on those previously reported.[11d]

***n*-Pentane in Silicalite.** Silicalite is the completely siliceous form of zeolite ZSM-5.[12] Unlike aluminum-containing zeolites which are hydrophilic, silicalite is hydrophobic and organophilic, and selectively adsorbs organic molecules over water. This characteristic property can be used to selectively adsorb nonpolar hydrocarbon molecules. Silicalite has a three-dimensional network of intersecting straight and zigzag channels.[12]

The Raman spectrum of *n*-pentane adsorbed in silicalite loaded with 8 molecules/unit cell (u.c.) at room temperature is shown in Figure 1C. An inspection of Figure 1A,C reveals some noticeable differences between the two spectra in the relative intensities for several bands associated with different conformers. Because the intensity of a Raman band due to a particular conformer is related to its concentration, the differences in intensity indicate that there are observable changes in the populations of the conformers. To better analyze the data, we removed the weak zeolite background in the region 1600−600 cm^{-1} by subtracting the Raman spectrum of calcined (unloaded) silicalite from the Raman spectrum of *n*-pentane/silicalite. The difference spectrum was then deconvoluted to separate the overlapping bands (Figure 2B). For comparison, the deconvoluted pure *n*-pentane spectrum in the same region is also shown in Figure 2A. Figure 2 and the normalized relative intensities for the selected Raman bands (Table 1) clearly illustrate that upon loading, the peaks assigned to the TT conformer gained intensity. The data indicate qualitatively that upon adsorption, the concentration of the TT conformer has increased. The changes in the relative intensities of the bands due to the TG conformers exhibit an opposite trend. Table 1 and Figure 2 show that the relative intensities of most bands belonging to the TG conformer decreased, suggesting that the adsorption in silicalite results in a decrease in the population of the TG conformer. Smit et al. simulated the adsorption of *n*-pentane in silicalite.[3b] Their calculated percentage of the *all-trans* conformer was found to be 63% and 55% for *n*-pentane located in the channels and channel intersections, respectively. The population of TT conformer at both locations is higher than is that of pure liquid (47%), which is qualitatively consistent with our experimental results. It appears that the dimension and geometry of the channel system in the silicalite structure prefer more *n*-pentane molecules to be oriented in nearly linear strings.

FT-Raman spectroscopy can also be used to probe the dynamics of *n*-pentane molecules within silicalite. It is well established that the line widths of certain Raman bands provide valuable information on the molecular dynamics.[13] Normally, the majority of the line widths of vibrational bands for small organic molecules in solution or liquid are much wider than those in the ordered solids due to molecular tumbling.[14] In the present case, loading *n*-pentane into silicalite did not result in

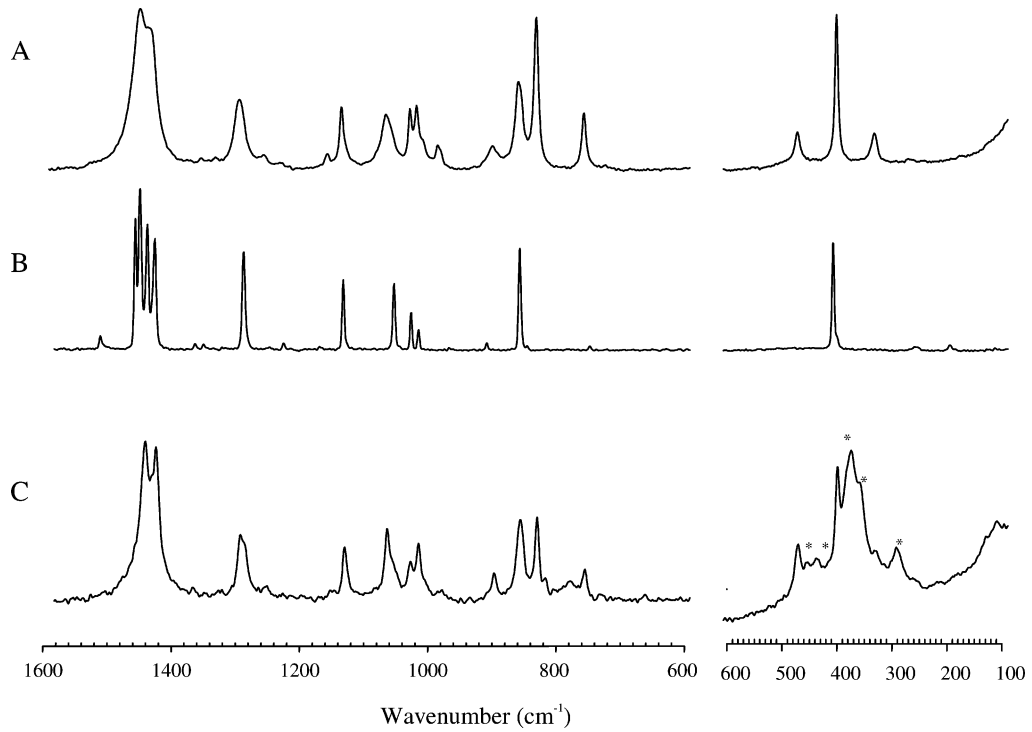

Figure 1. FT-Raman spectra of (A) pure liquid *n*-pentane at 298 K, (B) pure *n*-pentane at 140 K, and (C) *n*-pentane/silicalite (8 molecules/u.c.) at 298 K. The peaks labeled with an asterisk are due to zeolite framework vibrations.

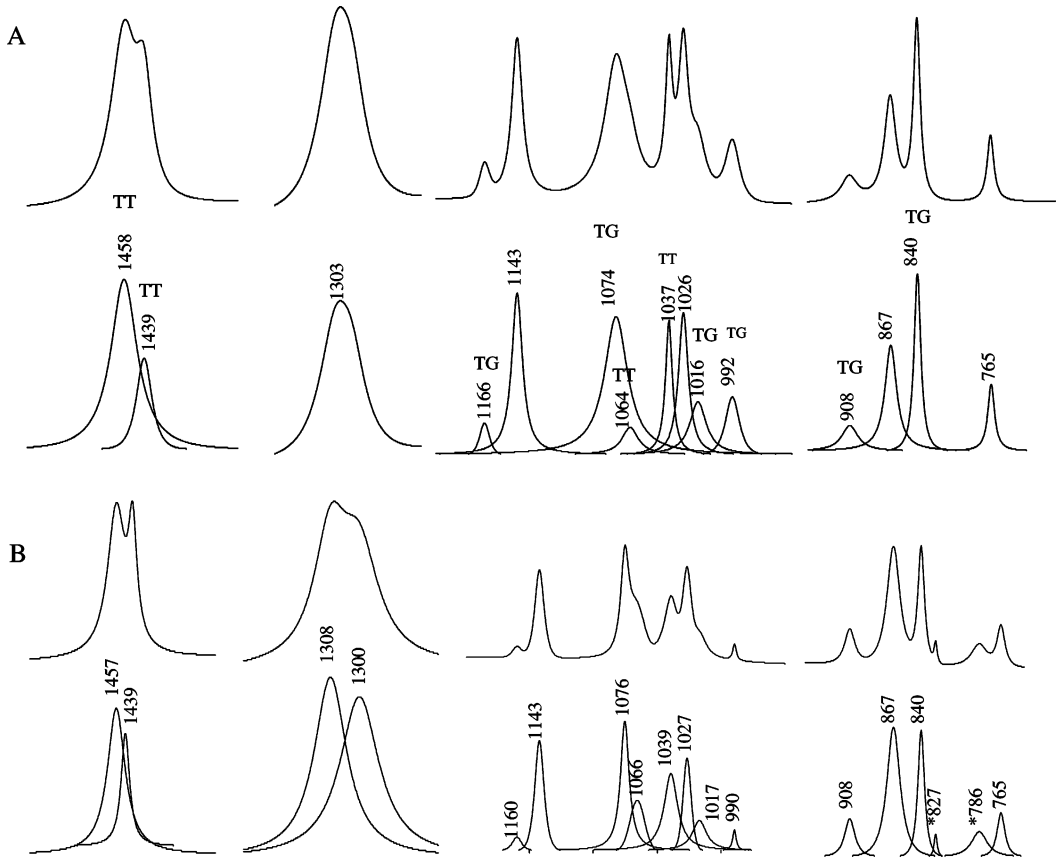

Figure 2. Deconvoluted FT-Raman spectra at 298 K in the region 1600−600 cm^{-1} of (A) pure liquid *n*-pentane and (B) *n*-pentane/silicalite (8 molecules/u.c.) with zeolite background being subtracted. The peaks labeled with an asterisk are due to residual zeolite framework vibrations.

dramatic line narrowing of the Raman bands compared to pure liquid. When the *n*-pentane/silicalite system is cooled to 153 K, several Raman bands have steadily decreased in their full width at half-height (fwhh) relative to the room temperature spectrum. For example, Figure 3B shows that although the two bands at 867 and 840 cm^{-1} have different fwhh, the line widths of both peaks gradually decrease with decreasing temperature. The observed changes are similar to those observed for pure liquid *n*-pentane (Figure 3A). These results clearly indicate that at room temperature the adsorbed *n*-pentane molecules retain a

TABLE 1: Normalized Peak Intensities[a] of the Selected Raman Bands Representing Different Conformers of *n*-Pentane Adsorbed in Silicalite at 298 K

			intensity (%)	
conformer	freq (cm^{-1})	assignments	pure liquid *n*-pentane	*n*-pentane/silicalite (8 molecules/u.c.)
TT	1458	CH_3 deform	32.5	37.3
	1439	CH_2 scissor	9.5	14.4
	1064	CC stretch	1.2	2.1
	1037	CC stretch	2.7	4.3
TG	1166	CH_2 rock	0.6	0.4
	1074	CC stretch	8.4	4.7
	1016	CH_3 rock	1.9	1.7
	992	CC stretch	1.6	0.3
	908	CH_3 rock	3.6	2.3
	840	CC stretch	9.7	5.0

[a] The intensity of each Raman band was normalized by dividing its intensity by the total integrated intensity in the region 1600−600 cm^{-1}.

substantial degree of molecular motion within the zeolite host. As the temperature is lowered, however, the degree of molecular motion is gradually reduced.

The locations of *n*-pentane molecules inside silicalite have been controversial. The silicalite framework contains two intersecting channel systems. The elliptical straight channel has a dimension of 5.75 × 5.14 Å, while the circular zigzag channel has a diameter of 5.5 Å.[12] The channel intersections have a near spherical cavity with a diameter of about 8.7 Å.[15] The kinetic diameter of *n*-pentane is 4.3 Å.[16] Silicalite is known to have three possible adsorption sites: the intersections between the straight and zigzag channels, and the midsections of the straight channels and zigzag channel segments. There are four equivalent positions for each site per unit cell. At the present time, there seems to be no consensus in the literature on the locations of *n*-pentane inside the silicalite framework. Jacobs[4h] and Thamm[4i] concluded that there is no preferential adsorption site for *n*-pentane in silicalite. The results of simulation by Titiloye et al.[3a] suggested that for *n*-pentane, the most preferred adsorption site is the channel intersection, and that the straight channel is slightly more favored than the zigzag channel. The work of Smit et al [3b] indicated that the straight and zigzag channels are equally available for adsorption and are more preferred than the channel intersection. They further calculated the distribution of *n*-pentane over the three adsorption sites at room temperature to be 49%, 44%, and 7% for zigzag, straight, and intersection, respectively.

The TGA curve (Figure 4A) exhibits a broad desorption peak centered at 105 °C with an obvious shoulder at 52 °C, corresponding to 6.91 and 0.81 molecules/u.c., respectively. To understand this result, we also obtained the TGA data of *n*-pentane adsorbed by siliceous Y (Si−Y) (Figure 4C). The TGA curve exhibits a single sharp peak. Silicalite and Si−Y both have a siliceous framework with no cations, therefore the interaction with nonpolar *n*-pentane is van der Waals in nature. Unlike silicalite that has three distinct adsorption sites, in Si−Y pentane molecules can only be adsorbed in a single cage (i.e., the supercage). This is why desorption of *n*-pentane from Si−Y yields only a single, narrow peak in the TGA curve. Thus, the broad desorption envelope observed for *n*-pentane/silicalite is likely due to two overlapping peaks originating from pentane molecules desorbed from two adsorption sites with similar energies. It seems that the *n*-pentane molecules adsorbed in silicalite are distributed over three different adsorption sites: The desorption peak appearing as a distinct shoulder at 52 °C, is due to an adsorption site accommodating 10.5% of the pentane in silicalite. Apparently, this site is energetically less favorable for adsorption as it only holds a small fraction of the adsorbed molecules that desorb at low temperature resulting from a weaker interaction with the framework. The broad profile centered at around 105 °C represents two overlapping peaks resulting from desorption of 89.5% of the total pentane molecules from two adsorption sites. The fact that the two desorption peaks were not resolved implies that both sites are almost equally preferred for pentane adsorption. From the earlier discussion, we know these three adsorption sites correspond to the straight and zigzag channels as well as the channel intersections. The TGA data alone, however, do not allow one to correlate the desorption peaks to specific adsorption sites. The Raman spectra, on the other hand, can provide useful insight in this regard. The information regarding the location of the guest molecules comes from the behavior of the Raman band at 1303 cm^{-1} seen in the spectrum of pure liquid pentane. This peak was assigned previously to the CH_2 twist modes of TT and TG conformers, which are accidentally degenerate.[11d] Upon loading an obvious shoulder appeared and the deconvoluted spectrum (Figure 2B) reveals clearly two separate peaks at 1308 and 1300 cm^{-1}. In general, the splitting may be due to several reasons: (1) correlation coupling due to sorbate−sorbate interaction, (2) removal of accidental degeneracy if the framework interacts with the TT and TG conformers differently, and (3) nonequivalent pentane molecules residing at different adsorption sites. The first possibility can be ruled out easily because the Raman spectrum of *n*-pentane solid at 140 K (Figure 1B) shows that this band did not spilt, suggesting that this particular mode does not undergo strong correlation splitting, even in solids. The second possibility is also unlikely since this band remains as a singlet in the Raman spectra of *n*-pentane adsorbed in zeolite hosts where there is only a single cage or channel for adsorption such as zeolites Na−Y, Si−Y, and L (Figures 5B and 6). Thus, the Raman data imply that the splitting originates from the *n*-pentane molecules located at different sites in silicalite. We further assign the peak at 1308 cm^{-1} to pentane molecules sitting in the middle sections of straight and zigzag channels and the band at 1300 cm^{-1} to guest molecules residing at the channel intersections. The assignments were based on the previous work, which has demonstrated that when a given guest molecule is located in either the zigzag or straight channel of the silicalite framework, certain vibrational modes may appear at higher frequency compared to molecule residing in the channel intersection.[6a] This is because the dimensions of zigzag and straight channels are significantly smaller than the diameter of channel interaction, resulting in the "tighter fit" of the guest molecule in the segment of the channels. Consequently, the vibrations of a guest molecule adsorbed in these sites are much more restricted by the surrounding framework, leading to a frequency shift toward higher energy (a phenomenon first reported by Dutta et al.[17]). In the present case, the frequency of the higher energy component is higher than that of pure liquid. We believe that for this bending mode, the stronger confinement on the encaged *n*-pentane molecules imposed by the zigzag and straight channels induces a slight change in the bond angles from the average values in a free molecule. This change increases resorting potential and therefore the energy of the bending mode. The reason that we assign the low-energy component to the *n*-pentane molecules located at the channel intersection is due to the fact that the frequency of this component is close to that of liquid pentane. The dimension of the channel intersection is larger compared to that of the molecule, which results in little vibrational perturbation from the surrounding framework. The intensity ratio of I_{1308}/I_{1300} is around 1.14, suggesting that 53% of pentane molecules are

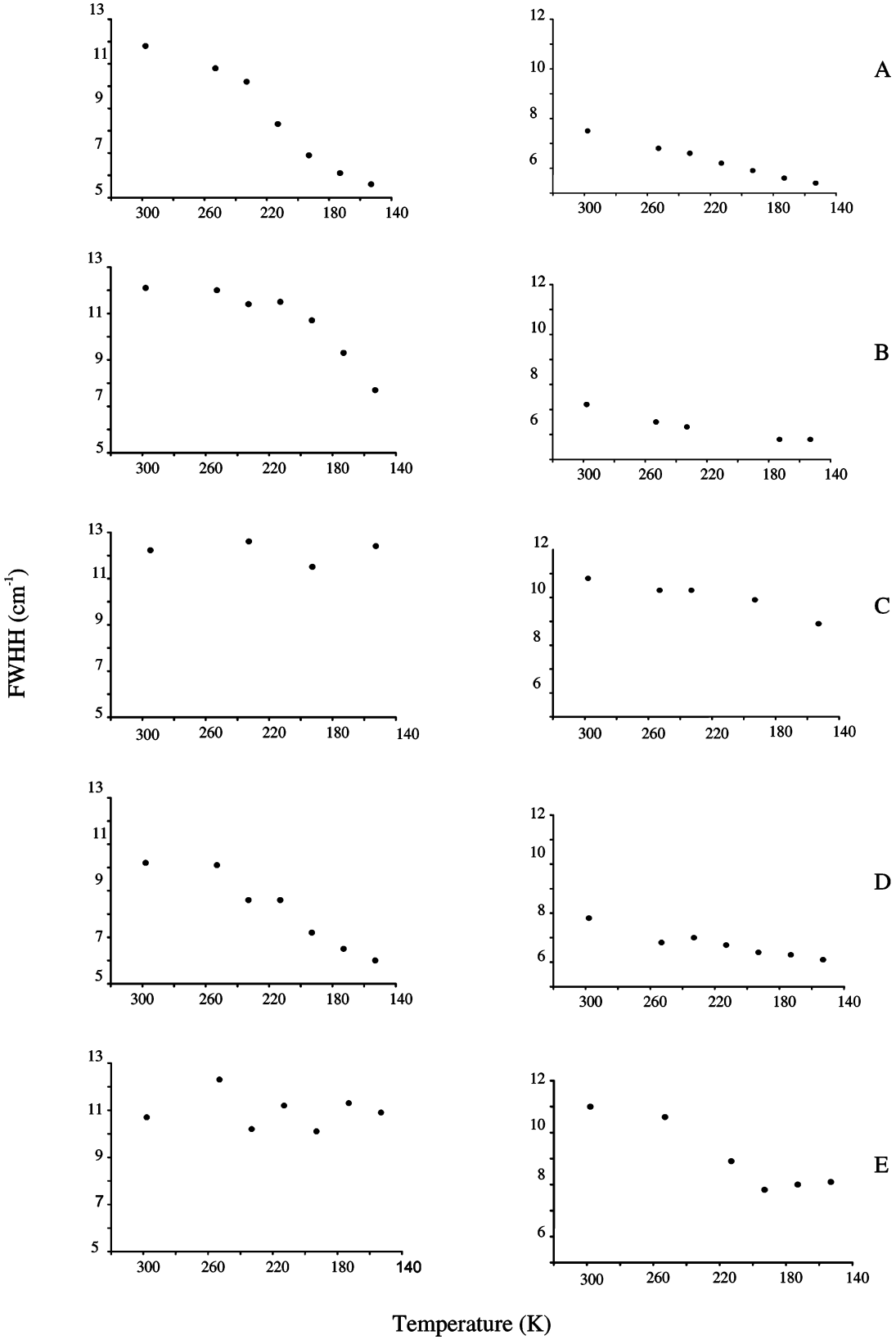

Figure 3. fwhh of the peaks of *n*-pentane as a function of temperature at 867 (left) and 840 cm^{-1} (right): (A) pure *n*-pentane; (B) *n*-pentane/silicalite (8 molecules/u.c.); (C) *n*-pentane/L (3 molecules/u.c.); (D) *n*-pentane/Si−Y (3 molecules/s.c); and (E) *n*-pentane/Na−Y (3 molecules/s.c).

located in zigzag and straight channels whereas 47% of the guest molecules are at the channel intersections. As discussed earlier, TGA data indicate that about 10% of pentane molecules are adsorbed at a high-energy site, which desorbed at lower temperature, while the rest of the guest molecules are at two sites with very similar energies. Assuming pentane molecules are equally populated in these two lower energy sites, the TGA and Raman data indicate that at a true loading of 7.71 molecules/u.c., on average, 3.46 pentane molecules (44.8% of the total sorbates) are located in the channel intersection (which is one of the sites with lower energy). The sites at straight and zigzag channels must have different energy and the low-energy site is

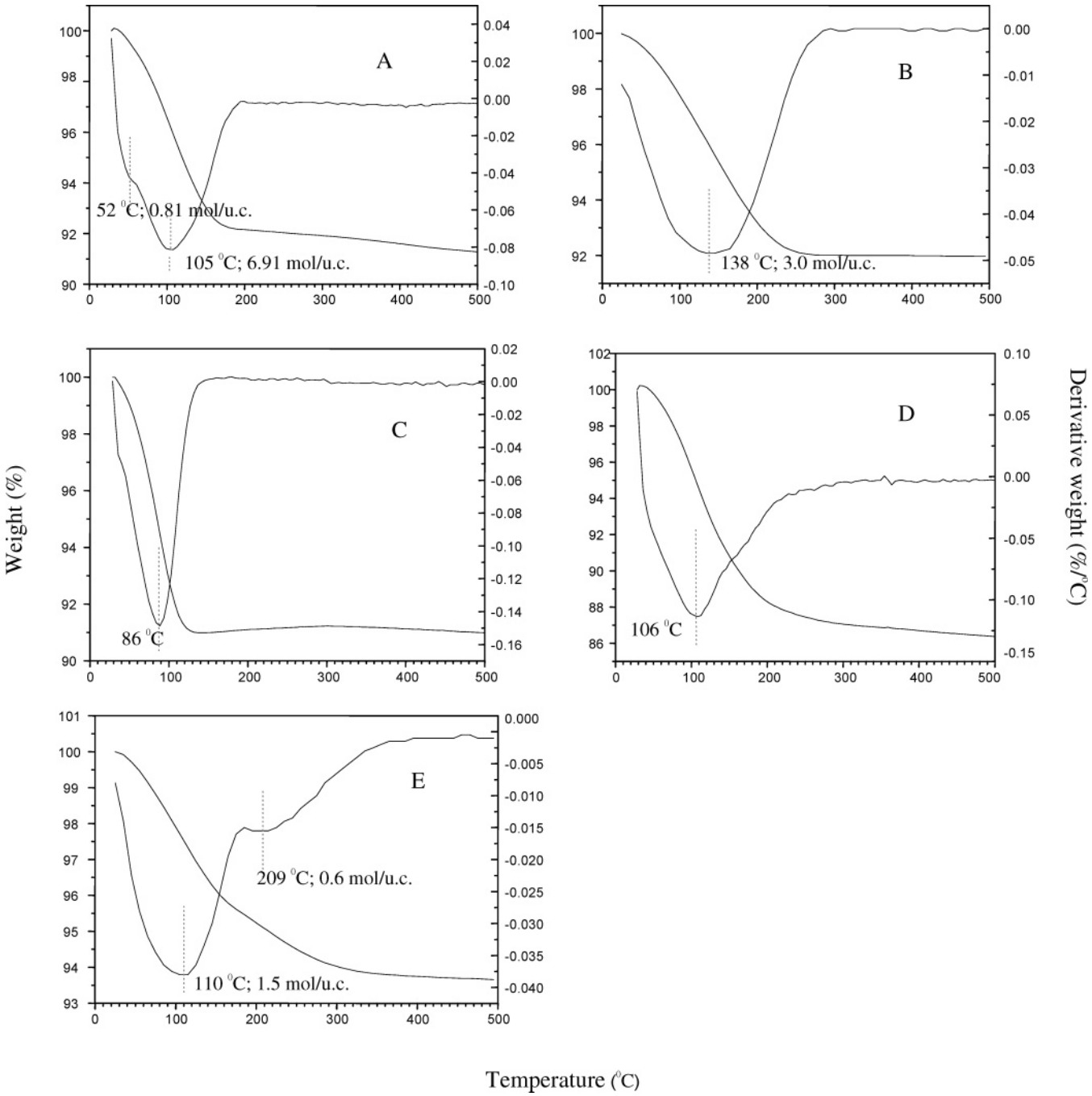

Figure 4. TGA curves of (A) *n*-pentane/silicalite (8 molecules/u.c.), (B) *n*-pentane/L (3 molecules/u.c.), (C) *n*-pentane/Si−Y (3 molecules/s.c.), (D) *n*-pentane/Na−Y (3 molecules/s.c.), and (E) *n*-pentane/ferrierite (2 molecules/u.c.).

occupied by 3.46 molecules and the higher energy site accommodates only 0.81 molecules. Unfortunately, the present study cannot distinguish one site from the other.

Silicalite is known to undergo phase transition upon adsorption of certain organic molecules.[18] We measured powder X-ray diffraction patterns of *n*-pentane/silicalite with different loading levels (not shown). The results indicated that adsorption of *n*-pentane did not induce any phase transition, even at the maximum loading level.

***n*-Pentane in Zeolite L.** Zeolite L has a one-dimensional channel system, which is characterized by a 7.1 Å diameter opening of a 12-membered ring.[19]

Figure 5B shows the Raman spectrum of *n*-pentane/L at a maximum loading level of 3 molecules/u.c. at room temperature. Similar to *n*-pentane/silicalite, the relative intensities of the peaks due to the TT conformer (such as the band at 1037 cm^{-1}) increased and those of the peaks associated with the TG conformer (e.g., the band at 840 cm^{-1}) decreased when *n*-pentane adsorbed in zeolite L. Upon cooling, further changes in relative intensities associated with different conformers were observed. To better monitor the change as a function of temperature, the relative intensity of the Raman bands originating from the pentane was calculated by using the zeolite peak at 500 cm^{-1} as an internal reference (Table 2). The intensity data shown in Table 2 indicate that intensities of the peaks associated with the TT conformer increased with decreasing temperature. For example, the relative intensities of the peaks at 1460, 1443, and 1067 cm^{-1} due to the TT conformer increased from 0.39, 0.35, and 0.05 at room temperature to 0.46, 0.48, and 0.14 at 153 K, respectively. The results indicate that

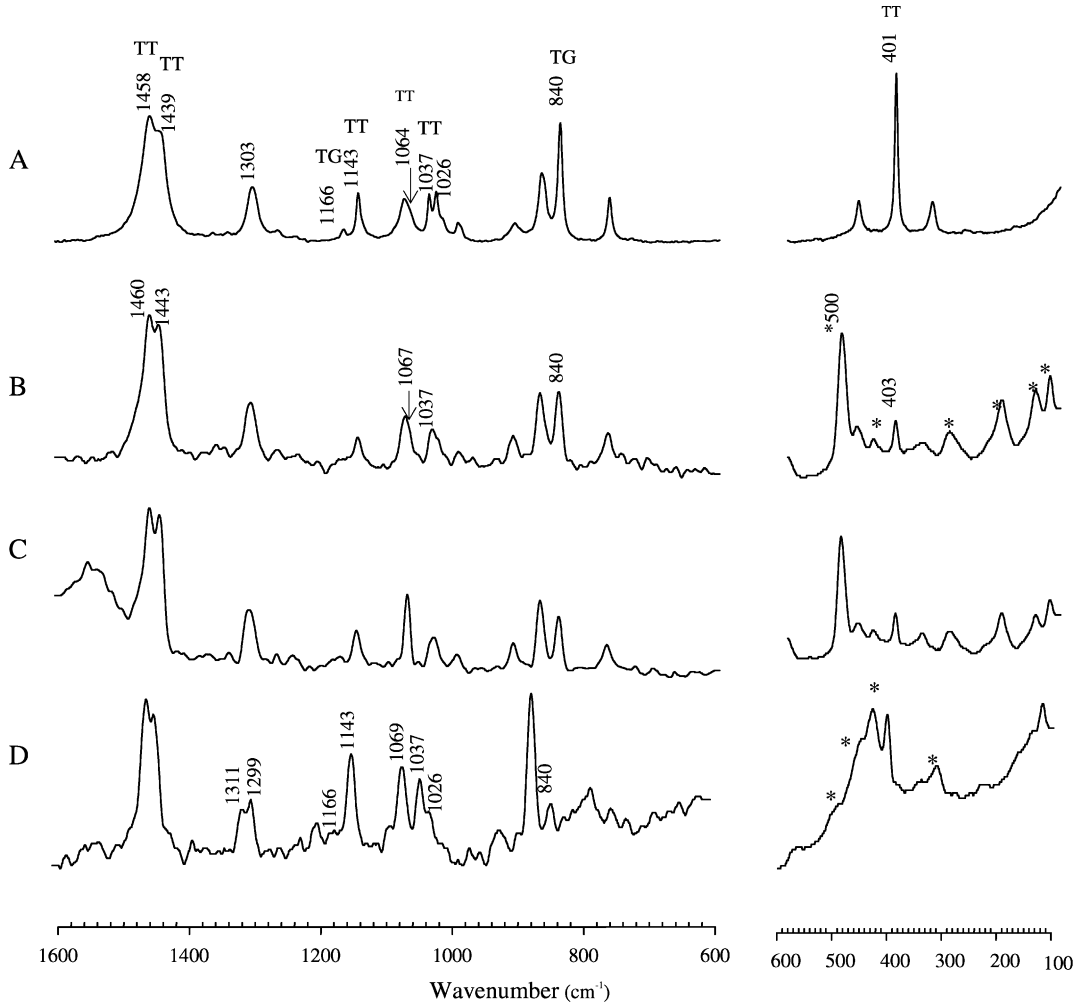

Figure 5. FT-Raman spectra of (A) pure liquid *n*-pentane at 298 K, (B) *n*-pentane/L (3 molecules/u.c.) at 298 K, (C) *n*-pentane/L (3 molecules/u.c.) at 153 K, and (D) *n*-pentane/ferrierite (2 molecules/u.c.) at 298 K. The peaks labeled with an asterisk are due to zeolite framework vibrations.

TABLE 2: Peak Intensities of the Selected Raman Bands Representing Different Conformers of *n*-Pentane/Zeolites[a]

	n-pentane/L (3 molecules/u.c.)			*n*-pentane/Si−Y (3 molecules/s.c.)			*n*-pentane/Na−Y (3 molecules/s.c.)		
	freq (cm^{-1})	298 K	153 K	freq (cm^{-1})	298 K	153 K	freq (cm^{-1})	298 K	153 K
TT	1460	0.39	0.46	1458	0.83	0.84	1459	0.85	1.03
TT	1443	0.35	0.48	1439	0.35	0.36	1441	0.23	0.48
TT	1144	0.07	0.07	1143	0.09	0.15	1143	0.13	0.19
TT	1067	0.05	0.14	1064	0.08	0.20	1064	0.10	0.20
TT	1032	0.08	0.05	1036	0.08	0.10	1036	0.08	0.12
TT	403	0.19	0.21	401	0.15	0.31	400	0.17	0.34
TG	1169	0.02	0.01	1166	0.01	*b*	1163	*b*	*b*
TG	1075	0.09	*b*	1074	0.15	0.06	1072	0.26	0.09
TG	1014	0.01	*b*	1015	0.03	*b*	1014	0.04	0.02
TG	992	0.03	0.03	989	0.06	*b*	993	0.06	0.03
TG	910	0.06	0.06	907	0.05	0.02	910	0.08	0.04
TG	842	0.15	0.12	839	0.21	0.12	840	0.26	0.10

[a] Raman peak intensity was normalized by dividing its intensity by the zeolite peak intensity. The peaks of zeolites L, Si−Y, and Na−Y are at 500, 507, and 502 cm^{-1}, respectively. [b] The intensities are too weak to measure.

the conformational equilibrium further shifted toward the TT conformer upon lowering the temperature.

It is interesting to note that the line widths of certain Raman modes such as the peak at 840 cm^{-1} (C−C stretch) increased upon loading and the line width of this and many other Raman bands did not decrease upon cooling (Figure 3C). As mentioned before, the vibrational bands of a small organic molecule in liquids are usually broad due to extensive molecular tumbling and the line width decreases upon lowering the temperature as the degree of the motion is reduced.[14] Compared to liquid, the degree of motion for the *n*-pentane molecules adsorbed in a zeolite should be reduced due to the spatial confinement imposed by the framework. Therefore, the increase in line width upon adsorption is unlikely due to a dynamic process. This coupled with the temperature independence of the line width for most Raman bands suggests the lack of significant molecular motion associated with *n*-pentane and that *n*-pentane molecules adsorbed in zeolite L are likely statically disordered. The extraframework cations in zeolite L are K^+. For the zeolite L used (Si/Al = 3.05) there are 8.9 K^+ per unit cell occupying four cation positions.[20] The presence of large K^+ ions in the 12-ring channel (site D) reduces the effective channel dimension.[21] It appears

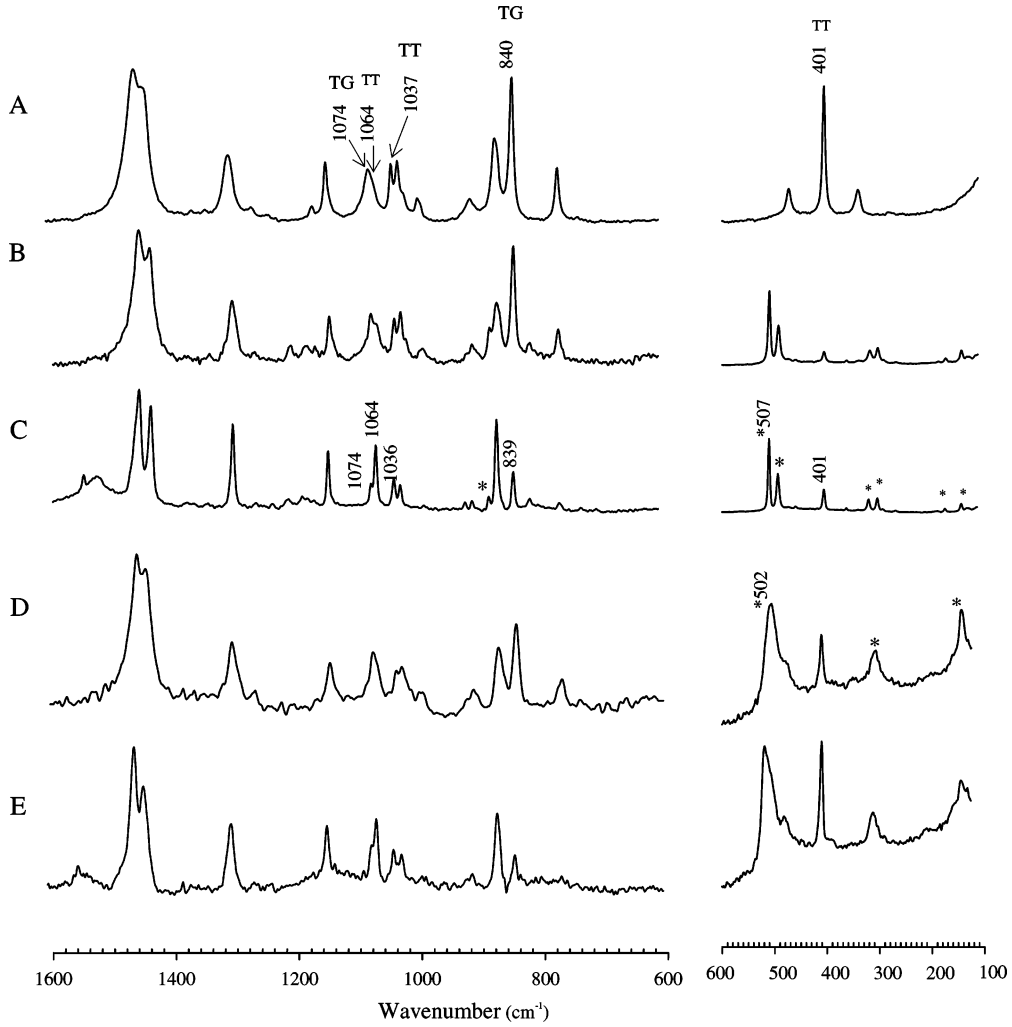

Figure 6. FT-Raman spectra of (A) pure liquid *n*-pentane at 298 K, (B) *n*-pentane/Si−Y (3 molecules/s.c.) at 298 K, (C) *n*-pentane/Si−Y (3 molecules/s.c.) at 153 K, (B) *n*-pentane/Na−Y (3 molecules./s.c.) at 298 K, and (C) *n*-pentane/Na−Y (3 molecules/s.c.) at 153 K. The peaks labeled with an asterisk are due to zeolite framework vibrations.

that inside the 12-ring channel, the *n*-pentane molecules are packed rather tightly at the maximum loading, resulting in little degree of motion. The guest molecules might have different orientations with respect to each other in the same channel and the orientations of *n*-pentane may also vary from channel to channel. Consequently, the recorded broad Raman spectrum is a cumulative average of all possible orientations of *n*-pentane molecules within the framework. The possible cation−guest interaction may also contribute to the reduced mobility of pentane in the framework. The TGA curve exhibits a very broad desorption peak (Figure 4B). Observation of a single peak is consistent with all pentane molecules being adsorbed in the 12-ring channels. The broadness of the peak supports the arguments that the distribution of the guest molecules in the framework might be somewhat disordered and the high desorption temperature may result from interactions between the guest molecules and cations.

***n*-Pentane in Faujasite Zeolites.** The next group of zeolites belongs to the faujasite family. It includes two zeolites that have identical (FAU) framework topology: siliceous Y (Si−Y) and Na−Y with a Si/Al ratio of 100 and 2.35, respectively. The framework of Faujasite zeolites consists of large α cages and smaller β cages. The α cage commonly referred to as a supercage is a nearly spherical cavity with a diameter of 12.5 Å, and the guest molecules can access this cage through a 12-ring window having a diameter of 7.4 Å. This is the cage where *n*-pentane molecules are adsorbed. The β cage also called the sodalite cage is not accessible for *n*-pentane molecules, simply because the 6-ring window is too small.[22]

The Raman spectrum of *n*-pentane/Si−Y at a loading level of 3 molecules/supercage (s.c.) at room temperature (Figure 6B) looked very similar to that of pure liquid *n*-pentane, indicating that the distribution of different conformers inside Si−Y is very similar to that of pure liquid *n*-pentane. The TGA curve (Figure 4C) contains only a single desorption peak at 86 °C. The narrowness of the peak and the low desorption temperature clearly indicate that all the pentane molecules are adsorbed in the supercage and that the interaction between the guest molecule and siliceous framework is fairly weak. The theoretical work by Bates et al. showed that the conformational behavior of *n*-pentane in Si−Y is very similar to that found in the gas phase,[3d] which is consistent with our experimental data. It seems that the large α cage does not impose a strong confinement on *n*-pentane to force significant conformational changes. These results differ from those of the *n*-pentane/silicalite system discussed earlier, which reflects the differences in the framework structure.

As the temperature of *n*-pentane/Si−Y was lowered, changes in the relative intensities of the Raman bands due to *n*-pentane were observed. Figure 6C shows that compared to the sharp zeolite peak at 507 cm^{-1}, the intensity of the pentane peaks due to the TT conformer centered at 1064, 1036, and 401 cm^{-1}

increased, and the peaks at 1074 and 839 cm^{-1} due to the TG conformer became much weaker upon cooling to 153 K. We further calculated the relative intensity for the Raman bands due to different pentane conformers by using the zeolite peak at 507 cm^{-1} as an internal standard reference (Table 2). All the results show that the population of the TT conformer increased at 153 K. It is worth noting that the changes in both the Raman intensities (Figure 6C) and the line width of *n*-pentane in Si−Y (Figure 3D) upon lowering the temperature are similar to those of pure liquid *n*-pentane, indicating that the larger α cage of Si−Y imposes little confinement on *n*-pentane molecules.

To examine the effect of the extraframework cations within the FAU framework on *n*-pentane conformation, we also obtained the Raman spectra of *n*-pentane/Na−Y at a loading level of 3 molecules/s.c. (Figure 6D,E). Na−Y has the same framework as Si−Y but contains a larger number of Na^+ ions. The Raman spectrum of *n*-pentane in Na−Y and its change with temperature are similar to those in Si−Y. It appears that the presence of the Na^+ ion in the α-cage does not strongly affect the conformational behavior of the nonpolar *n*-pentane molecule.

Interestingly, the dynamic behavior of *n*-pentane in Si−Y and Na−Y is quite different. Figure 3D shows that for *n*-pentane in Si−Y, the line width gradually decreases with lowering temperature and this trend is almost identical with that for *n*-pentane in silicalite. For the *n*-pentane/Na−Y system, the situation is different (Figure 3E). The temperature dependence of the line width for the same Raman bands in Na−Y is actually rather similar to those in zeolite L. These results indicate that *n*-pentane in Si−Y undergoes extensive motion, but inside Na−Y, the degree of the overall motion is drastically reduced. The TGA curve of *n*-pentane/Na−Y shows a single peak (Figure 4D). Compared to *n*-pentane/Si−Y, the desorption peak is much broader and the desorption temperature (106 °C) is 20 °C higher. As mentioned earlier, both Si−Y and Na−Y have the same framework topology, and the major difference is the presence of cations in Na−Y. Although *n*-pentane is a nonpolar molecule, the Raman and TGA data clearly indicate that the presence of sodium ions in the framework does affect its dynamics and desorption temperature.

***n*-Pentane in Ferrierite.** Ferrierite is an aluminosilicate with two straight, elliptical channels. The 10-ring channel of pore diameter 5.4 × 4.2 Å are interconnected with an 8-ring channel of diameter 4.8 × 3.5 Å.[23] Ferrierite has been used as a shape selective catalyst for the production of isobutene in the petrochemical industry.[24]

The Raman spectrum of *n*-pentane adsorbed in zeolite ferrierite loaded with 2 molecules/u.c. at room temperature is shown in Figure 5D. Upon loading, the intensities of the peaks associated with the TT conformer increased dramatically. For instance there is a significant increase in the intensity of the peaks at 1069 and 1037 cm^{-1} (both due to the TT conformer) when *n*-pentane is adsorbed in ferrierite. On the other hand, there is a marked decrease in the intensity of the bands due to the TG conformer. For example, the very strong peak at 840 cm^{-1} seen in pure *n*-pentane became extremely weak upon loading. Our data agree with a computational study that predicted that for *n*-alkanes the isomers with *trans* conformations are favored in ferrierite.[3d] The changes in intensity for *n*-pentane/ferrierite at room temperature are the largest among all the zeolites examined, implying that ferrierite strongly favors the TT conformation. This is due to the fact that the channels in ferrierite have the smallest dimensions among all the zeolites.

The band at 1303 cm^{-1} in pure liquid *n*-pentane split into two components upon adsorption. On the basis of the discussion for the *n*-pentane/silicalite system, we suggest that the splitting is due to the existence of two nonequivalent *n*-pentane molecules. The pentane molecules corresponding to the high-frequency component of the doublet must reside in a highly restricted environment since this band is 12 wavenumbers higher in frequency compared to the low-frequency component. We suggest that the high-frequency component represents the pentane molecules located in the 8-ring channel, which is less accommodating, and the low-frequency component corresponds to the pentane molecules residing in the 10-ring channel. The TGA curve of *n*-pentane/ferrierite exhibits two desorption peaks at 110 (1.5 molecules/u.c.) and 209 °C (0.6 molecules/u.c.), respectively (Figure 4E), confirming the existence of two different types of pentane molecules, residing in the 8- and 10-ring channels, respectively. Thus, both Raman and TGA results indicate that there are two adsorption sites for *n*-pentane in ferrierite. Our result is also consistent with a previous ^{13}C CP MAS NMR study, which indicated that *n*-pentane molecules preferentially occupy the 10-ring channels at a loading of 1.6 molecules/u.c. or less, and adsorption into the 8-ring channel occurs only at higher loadings.[5b]

Summary

The adsorption of *n*-pentane inside zeolites silicalite, ferrierite, L, Si−Y, and Na−Y was examined by FT-Raman spectroscopy and thermogravimetric analysis. The framework topology appears to determine the conformation of the sorbed *n*-pentane molecules. For the zeolites with channel systems such as silicalite, ferrierite, and zeolite L, upon adsorption into the channels at room temperature, the population of the TT conformer clearly increases, resulting from the fact that the geometry of this isomer fits better in the channel. For *n*-pentane adsorbed in zeolites with large cavities such as Si−Y and Na−Y, the distribution of various conformers and its temperature dependence are more similar to those of pure liquid, suggesting the large supercage in the framework imposes only minimum effect on the conformational equilibriums.

The dynamics of the guest molecule is affected remarkably by the existence of charge balancing cations. For the *n*-pentane adsorbed in a siliceous framework such as silicalite and Si−Y, extensive molecular motion was detected at room temperature and the degree of the motion decreases with decreasing temperature. In zeolites L and Na−Y, the presence of cations in the framework hindered the overall molecular motion. The cations clearly interact with the *n*-pentane molecule, which may contribute, at least partially, to the static disorder of the guest molecule in zeolite L.

Important information regarding the location of *n*-pentane molecules within silicalite and ferrierite was also obtained.

Acknowledgment. Y.H. acknowledges the financial support from the Natural Science and Engineering Research Council of Canada for a research and an equipment grant. Funding from the Canada Research Chair and Premier's Research Excellence Award programs is also gratefully acknowledged.

References and Notes

(1) Dyer, A. *An Introduction to Zeolite Molecular Sieves*; John Wiley & Sons: Chichester, UK, 1988; pp 1 and 2.

(2) Furtado, E. A.; Chaer Nascimento, M. A. In *Theoretical Aspects of Heterogeneous Catalysis*; Chaer Nascimento, M. A., Ed.; Kluwer Academic Publishers: Dordrecht, The Netherlands, 2001; pp 39−76.

(3) (a) Titiloye, J. O.; Parker, S. C.; Stone, F. S.; Catlow, C. R. A. *J. Phys. Chem.* **1991**, *95*, 4038−4044. (b) Smit, B.; Siepmann, J. I. *J. Phys. Chem.* **1994**, *98*, 8442−8452. (c) Bates, S. P.; van Well, W. J. M.; van Santen, R. A.; Smit, B. *J. Am. Chem. Soc.* **1996**, *118*, 6753−6759. (d) Bates,

S. P.; van Well, W. J. M.; van Santen, R. A.; Smit, B. *J. Phys. Chem.* **1996**, *100*, 17573−17581. (e) Rajappa, C.; Bandyopadhyay, S.; Subramanian, Y. *Bull. Mater. Sci.* **1997**, *20*, 8845−878. (f) Vlugt, T. J. H.; Krishna, R.; Smit, B. *J. Phys. Chem. B* **1999**, *103*, 1102−1118. (g) Pascual, P.; Boutin, A. *Phys. Chem. Chem. Phys.* **2004**, *6*, 2015−2017. (h) Loisruangsin, A.; Fritzsche, S.; Hannongbua, S. *Chem. Phys. Lett.* **2004**, *390*, 485−490. (i) Calero, S.; Dubbeldam, D.; Krishna, R.; Smit, B.; Vlugt, T. J. H.; Denayer, J. F. M.; Martens, J. A.; Maesen, T. L. M. *J. Am. Chem. Soc.* **2004**, *126*, 11377−11386. (j) Fuchs, A. H.; Cheetham, A. K. *J. Phys. Chem. B* **2001**, *105*, 7375−7383.

(4) (a) van Well, W. J. M.; Wolthuizen, J. P.; Smit, B.; van Hooff, J. H. C.; van Santen, R. A. *Angew. Chem., Int. Ed. Engl.* **1995**, *34*, 2543−2544. (b) Sun, M. S.; Talu, O.; Shah, D. B. *J. Phys. Chem.* **1996**, *100*, 17276−17280. (c) Long, Y.; Jiang, H.; Zeng, H. *Langmuir* **1997**, *13*, 4094−4101. (d) Denayer, J. F.; Baron, G. V.; Martens, J. A.; Jacobs, P. A. *J. Phys. Chem. B* **1998**, *102*, 3077−3081. (e) Millot, B.; Methivier, A.; Jobic, H. *J. Phys. Chem. B* **1998**, *102*, 3210−3215. (f) Denayer, J. F.; Souverijns, W.; Jacobs, P. A.; Martens, J. A.; Baron, G. V. *J. Phys. Chem. B* **1998**, *102*, 4588−4597. (g) Arik, I. C.; Denayer, J. F.; Baron, G. V. *Microporous Mesoporous Mater.* **2003**, *60*, 111−124. (h) Jacobs, P. A.; Beyer, H. K.; Valyon, J. *Zeolites* **1981**, *1*, 161−168 (i) Thamm, H. *Zeolites* **1987**, *7*, 341−346.

(5) (a) van Well, W. J. M.; Janchen, J.; de Haan, J. W.; van Santen, R. A. *J. Phys. Chem. B* **1999**, *103*, 1841−1853. (b) van Well, W. J. M.; Cottin, X.; de Haan, J. W.; Smit, B.; Nivarthy, G.; Lercher, J. A.; van Hooff, J. H. C.; van Santen, R. A. *J. Phys. Chem. B* **1998**, *102*, 3945−3951 (c) van Well, W. J. M.; Cottin, X.; Smit, B.; van Hooff, J. H. C.; van Santen, R. A. *J. Phys. Chem. B* **1998**, *102*, 3952−3958. (d) Huang, Y.; Wang, H. *Langmuir* **2003**, *19*, 9706−9713. (e) Morell, H.; Angermund, K.; Lewis, A. R.; Brouwer, D. H.; Fyfe, C. A.; Gies, H. *Chem. Mater.* **2002**, *14*, 2192−2198. (f) Mentzen, B. F.; Vedrine, J. C. *C. R. Acad. Sci.* **1985**, *301*, 1017−1120.

(6) (a) Huang, Y.; Havenga, E. A. *J. Phys. Chem. B* **2000**, *104*, 5084−5089. (b) Stair, P. C. *Curr. Opin. Solid State Mater. Sci.* **2001**, *5*, 365−369. (c) Crawford, M. K.; Dobbs, K. D.; Smalley, R. J.; Corbin, D. R.; Maliszewskyj, N.; Udoric, T. J.; Cavanagh, R. R.; Rush, J. J.; Grey, C. P. *J. Phys. Chem. B* **1999**, *103*, 431−434. (d) Huang, Y.; Leech, J. H. *J. Phys. Chem. B* **2003**, *107*, 7647−7653.

(7) Chase, D. B.; Rabolt, J. F. In *Fourier Transform Raman Spectroscopy From Concept to Experiment*; Chase, D. B., Rabolt, J. F., Eds.; Academic Press: San Diego, CA, 1994; pp 1−48.

(8) Robson, H. *Microporous Mesoporous Mater.* **1998**, *22*, 628−629.

(9) (a) Bartell, L. S.; Kohl, D. A. *J. Chem. Phys.* **1963**, *39*, 3097−3105. (b) Bonham, R. A.; Bartell, L. S.; Kohl, D. A. *J. Am. Chem. Soc.* **1959**, *81*, 4765−4769.

(10) (a) Almarza, N. G.; Enciso, E.; Bermejo, F. J. *J. Chem. Phys.* **1992**, *96*, 4625−4632. (b) Vega, C.; Lago, S.; Garzon, B. *J. Chem. Phys.* **1994**, *100*, 2182−2190. (c) Tsuzuki, S.; Uchimaru, T.; Tanabe, K. *Chem. Phys. Lett.* **1995**, *246*, 9−12.

(11) (a) Mizushima, S.; Simanouti, T. *J. Am. Chem. Soc.* **1949**, *71*, 1320−1324. (b) Sheppard, N.; Szasz, G. J. *J. Chem. Phys.* **1949**, *17*, 86−92. (c) Schaufele, R. F. *J. Chem. Phys.* **1968**, *49*, 4168−4175. (d) Harada, I.; Takeuchi, H.; Sakakibara, M.; Matsuura, H.; Shimanouchi, T. *Bull. Chem. Soc. Jpn.* **1977**, *50*, 102−110. (e) Kanesaka, I.; Synder, R. G.; Strauss, H. L. *J. Chem. Phys.* **1986**, *84*, 395−397. (f) Snyder, R. G.; Kim, Y. *J. Phys. Chem.* **1991**, *95*, 602−610. (g) Mirkin, N. G.; Krimm, S. *J. Phys. Chem.* **1993**, *97*, 13887−13895.

(12) (a) Flanigen, E. M.; Bennett, J. M.; Grose, R. W.; Cohen, J. P.; Patton, R. L.; Kirchner, R. M.; Smith, J. V. *Nature* **1978**, *271*, 512−516. (b) Kokotailo, G. T.; Lawton, S. L.; Olson, D. H.; Meier, W. M. *Nature* **1978**, *272*, 437−438.

(13) Hacura, A.; Zerda, T. W.; Kaczmarski, M. *J. Raman Spectrosc.* **1981**, *11*, 437−441.

(14) Sushchinskii, M. M. *Raman Spectra of Molecules and Crystals*; Israel Program for Scientific Translations: New York, 1972.

(15) Nowak, A. K.; Chectham, A. K.; Pickett, S. D. *Mol. Simul.* **1987**, *1*, 67−77.

(16) Breck, D. W. *Zeolite Molecular Sieves*; Wiley: New York, 1974; p 636.

(17) Dutta, P. K.; Delbarco, B.; Shieh, D. C. *Chem. Phys. Lett.* **1986**, *127*, 200−204.

(18) Fyfe, C. A.; Kennedy, G. J.; Kokotailo, G. T.; DeSchutter, C. T. *J. Chem. Soc., Chem. Commun.* **1984**, *16*, 1093−1094.

(19) Barrer, R. M.; Villiger, H. *Z. Kristallogr.* **1969**, *128*, 352−370.

(20) Newell, P. A.; Rees, L. V. C. *Zeolites* **1983**, *3*, 28−36.

(21) Newsam, J. M., *J. Phys. Chem.* **1989**, *93*, 7689−7694.

(22) Hopkins, P. D. *J. Catal.* **1973**, *29*, 112−119.

(23) (a) Vaughan, P. A. *Acta Crystallogr.* **1966**, *21*, 983−990. (b) Kerr, I. S. *Nature* **1966**, *210*, 294−295.

(24) Finelli, Z. R.; Querini, C. A.; Comelli, R. A. *Appl. Catal., A* **2003**, *247*, 143−156.